

Article

Not peer-reviewed version

Leucine-rich repeat in polycystin-1 suppresses cystogenesis in a zebrafish (*Danio rerio*) model of autosomal dominant polycystic kidney disease

[Biswajit Padhy](#)^{*}, Mohammad Amir, Jian Xie, [Chou-Long Huang](#)^{*}

Posted Date: 29 January 2024

doi: 10.20944/preprints202401.1959.v1

Keywords: Polycystin-1 protein, Polycystic kidney disease, Leucine-rich repeats, Laminin, Zebrafish.



Preprints.org is a free multidiscipline platform providing preprint service that is dedicated to making early versions of research outputs permanently available and citable. Preprints posted at Preprints.org appear in Web of Science, Crossref, Google Scholar, Scilit, Europe PMC.

Copyright: This is an open access article distributed under the Creative Commons Attribution License which permits unrestricted use, distribution, and reproduction in any medium, provided the original work is properly cited.

Article

Leucine-Rich Repeat in Polycystin-1 Suppresses Cystogenesis in a Zebrafish (*Danio rerio*) Model of Autosomal Dominant Polycystic Kidney Disease

Biswajit Padhy †; Mohammad Amir †; Jian Xie; and Chou-Long Huang

Department of Internal Medicine, Division of Nephrology, University of Iowa Carver College of Medicine, Iowa City, Iowa, USA.

* Correspondence: biswajit-padhy@uiowa.edu (B.P.); chou-long-huang@uiowa.edu

† These authors contributed equally to this work.

Abstract: Mutations of *PKD1* coding for polycystin-1 (PC1) account for most of the autosomal dominant polycystic kidney disease (ADPKD). The extracellular region of PC1 contains many evolutionarily conserved domains for ligand interactions. Among these is the leucine-rich repeats (LRR) in the far N-terminus of PC1. Using zebrafish (*Danio rerio*) as an *in vivo* model system, we explored the role of LRR in the function of PC1. Zebrafish expresses two human *PKD1* paralogs, *pkd1a* and *pkd1b*. Knockdown of both genes in zebrafish by morpholino antisense oligonucleotides produced phenotypes of dorsal axis curvature and pronephric cyst formation. We found that overexpression of LRR suppressed both phenotypes in *pkd1*-morphant zebrafish. Purified recombinant LRR domain inhibited proliferation of HEK cells in culture and interacted with the heterotrimeric basement membrane protein laminin-511 ($\alpha 5\beta 1\gamma 1$) in vitro. Mutations of amino acid residues in LRR structurally predicted to bind laminin-511 disrupted LRR-laminin interaction in vitro and neutralized the ability of LRR to inhibit cell proliferation and cystogenesis. Our data support the hypothesis that the extracellular region of PC1 plays a role in modulating PC1 interaction with the extracellular matrix and contributes to cystogenesis of PC1-deficiency.

Keywords: Polycystin-1 protein; Polycystic kidney disease; leucine-rich repeats; laminin; zebrafish

Introduction

Autosomal dominant polycystic kidney disease (ADPKD) is an inherited monogenic disorder diagnosed by renal cysts typically in the adults between ages of 30 and 50. ADPKD is an important cause of end-stage renal disease (ESRD) and apart from kidney cysts, it may lead to extrarenal complications like development of cysts in liver and pancreas, intracranial aneurysms, diverticulosis, and cardiovascular abnormalities. (1) Majority of ADPKD cases is due to mutations in the genes polycystic kidney disease 1 (*PKD1*) and polycystic kidney disease 2 (*PKD2*) that encodes for polycystin-1 (PC1) and polycystin-2 (PC2) protein, respectively. PC1 of which mutations causing ~80% of ADPKD cases, is an integral membrane bound protein localized to cilia, plasma membrane, desmosomal junctions, and endoplasmic reticulum (ER). (2-4) It consists of 4,303 amino acids containing a long extracellular N-terminus, 11-transmembrane domains, and a relatively shorter cytoplasmic C-terminus. PC2 is a Ca^{2+} -permeable non-selective cation channel.

The last six transmembrane (TM) segments of PC1 interacts with corresponding transmembrane segments of PC2 in a 1:3 stoichiometric ratio to form a PC1/PC2 heterotetramer polycystin channel complex. (5) The 226 amino acids long C-terminal tail of PC1 is shown to interact with multiple signaling proteins such as STAT6, P100, (6) heterotrimeric G-proteins (7) and AP-1 activation. (8) In addition, cytoplasmic C-terminal tail of PC1 is found to interact with the coiled-coil domain of PC2 which may regulate PC2 channel activity. (9, 10)

The extracellular N-terminal region of PC1 contains more than two-third of the PC1 protein (>3000 amino acids). There are seven distinct, evolutionarily conserved structural domains in the extracellular region of PC1, most of which are reported to be involved in cell-cell or cell-matrix interactions. (11) Association of PC1 and PC2 may allow PC2 to respond to external stimuli through the extracellular N-terminal region of PC1. Disturbances of these interaction may lead to

cystogenesis. However, the developmental and subcellular expression of PC1 and PC2 are not congruent. (2, 12-14) Thus, PC1 may work independently of PC2. To elucidate the function of extracellular region of PC1 in the progression of renal cystogenesis we employed zebrafish (ZF) (*Danio rerio*) as an *in vivo* model system for ADPKD. We show that cystic phenotypes in PC1-knocked down ZF embryos can be suppressed by transgenic overexpression of N-terminus leucine-rich repeats (LRR). We provide evidence that this is likely through LRR binding to laminin to modulate laminin-integrin interaction. The results support the notion that the extracellular region of PC1 plays an important role in anti-cystogenesis.

Materials and Methods

Cell Culture and Transfection

HEK293 cells were grown in Dulbecco's Modified Eagle Medium (Gibco, NY, USA), 10% fetal bovine serum (Gibco, NY, USA), 100 U/mL Pen Strep (Gibco, NY, USA) and 0.25 µg/mL Amphotericin B (Gibco, NY, USA) and maintained at 37°C and 5% CO₂. For plasmid transfections, Lipofectamine 2000 was used following manufacturer's instructions (ThermoFisher Scientific, Waltham, MA).

Plasmids, Site-Directed Mutagenesis, and in vitro RNA synthesis

pcDNA5-FRT-TO-PKD1-HA was generously provided by Dr. Julie Xia Zhou (University of Kansas Medical Center, Kansas City, KS). Targeted deletions and substitutions were introduced by Q5® Site-Directed Mutagenesis Kit (New England Biolabs, Ipswich, MA) according to the protocol provided by the manufacturer and validated by sequencing. Bases corresponding to amino acids 3075-4303 and 177-4303 were deleted from the *PKD1* full length cDNA sequence to create ECD (1-3074 a.a) and LRR (1-176 a.a) expressing plasmids, respectively. Subsequently, capped mRNAs were synthesized from enzyme digested linear constructs using HiScribe™ T7 In Vitro Transcription Kit following manufacturer's instructions (New England Biolabs, Ipswich, MA).

Zebrafish Housing and Morpholino (MO) Injection

Wild-type zebrafish (*Danio rerio*) were bred and maintained at 28°C in a 14-10 hr light-dark cycle. All procedures were followed in accordance with the approved protocols by the University of Iowa Animal care and Use committee. Experiments were performed as previously described. (15) Briefly, knockdown of zebrafish *pkd1a* and *pkd1b* genes were carried out by injecting previously validated gene specific antisense MO oligonucleotides (Gene Tools, LLC, Philomath, OR, USA). (16) At 1-4 cell stage, each fertilized eggs were microinjected with 2 ng of either *pkd1a* or *pkd1b* MO or both. In addition to MOs, embryos were injected with 200 pg of in vitro synthesized capped mRNAs or vehicle in a total volume of 4.6 nL by using a Nanoject microinjector (Drummond Scientific, Broomall, PA, USA). Injected embryos were incubated in egg water at 28°C and analyzed at 3 days post fertilization (dpf). For histological sectioning and staining, embryos at 3 dpf were fixed in 4% paraformaldehyde at 4°C overnight. Afterwards embryos were sequentially treated with 10% and 20% sucrose for 30 min each and then with 30% sucrose until it sinks to the bottom of the tube. Then embryos were fixed in a mold and embedded in optimal cutting temperature (OCT) medium and sectioned at 5 µm. Following Sullivan-Brown *et al.*, tissue sections were stained in Hematoxylin and Eosin stain and imaged on a Nikon Eclipse E600. (17)

Structure Refinement, Molecular Modeling, and Interaction Analysis

The atomic coordinates of Laminin-511 were retrieved from the Protein Data Bank (PDB ID: 5XAU). It consists of three chains, α5, β1, and γ1, which assemble into a cross-shaped heterotrimer. (18) For low density region or missing residues, the WT structure of Laminin-511 was modeled by MODELER 9.20 embedded in the PyMOL plugin PyMod 2.0 (www.pymol.org) using 5XAU as a template. LRR (24–176 aa) of PKD1 was used to generate a three-dimensional (3D) homology model

from multiple threading alignments and iterative structural assembly simulations using I-TASSER. (19, 20) I-TASSER homology modeling gives us five structures corresponding to the five largest structure clusters. The confidence of each model is quantitatively measured by its C-score (-5-2), where a model with a high C-score signifies a model with higher confidence and vice versa. We selected the LRR 3D atomic model with the highest C-score for our study. LRR WT structure was used to create E107A and W139C mutations using a mutagenesis plugin embedded in PyMOL. Mutants and WT structures of LRR were energy minimized using SPDBV to remove high-energy configurations by changing their coordinate geometries in such a way as to release internal constraints and reduce the total potential energy. The final energy-minimized structures of laminin-511 and LRRs (WT, E107A, and W139C) were used for blind docking using ClusPro2. (21) Protein-protein complexes produced by ClusPro2 are considered to have a high degree of confidence because it scored as the topmost protein-protein docking tool in the CAPRI assessment recently (<https://abcgroup.ClusPro2.org/2020/01/16/ClusPro2-ranks-first-in-the-7th-capri-evaluation-round/>).

Cloning, Expression, and Purification of LRRs

cDNA fragments encoding LRR (24–176 aa) were amplified using PCR and subcloned into the pGEX-4T-1 vector to generate GST fusion proteins. The expression vector harboring point mutations for LRR (E107A and W139C) was generated following the standard protocol of the Q5® Site-Directed Mutagenesis Kit (E0554S, New England Biolabs). The LRRs insert was confirmed by double digestion and DNA sequencing. Expression vectors were transformed and expressed into *Escherichia coli* BL21 DE3 cells. Cells were grown at 37°C and induced with 0.5 mM IPTG (Sigma, Saint Louis, USA) when absorbance reached 0.5–0.6 at 600 nm. Overnight grown cell culture was centrifuged at 4000g for 10 min at 4°C and pellets were dissolved in cell lysis buffer (50 mM Tris–HCl buffer, pH 8.0, 500 mM NaCl, 5 % (v/v) glycerol, 2 mM DTT, 0.1 mg/ml lysozyme, 5 mM phenyl methane sulfonyl fluoride (PMSF), 1 % (v/v) Triton X-100 (U.S. Biochemical Corp.), and 0.1% Tween-20). Sonication was used for cell lysis on ice for 10 min, and pellets (now called inclusion bodies; IBs) were collected after centrifugation for 30 min at 13,000 rpm at 4°C. IBs were washed three times with milli-Q water to get pure IBs. Further, IBs were solubilized with 0.3% N-lauroylsarcosine (sarcosine) overnight at room temperature to obtain a high amount of our solubilized protein. To remove sarcosine, sample was dialyzed overnight against buffer (50 mM Tris–HCl buffer, pH 8.0, 200 mM NaCl, and 1 mM DTT) at 4°C. The supernatant collected after centrifugation was filtered with a 0.22-um filter before loading to a glutathione affinity column equilibrated with buffer (50 mM Tris–HCl buffer, pH 8.0, 200 mM NaCl, and 1 mM DTT) to capture the GST-tagged LRR (GST-LRR). The column was then washed with wash buffer (50 mM Tris–HCl buffer, pH 8.0, 200 mM NaCl, and 1 mM DTT), and our target protein bound to resin was eluted in elution buffer in a stepwise manner, starting with wash buffer containing 5 mM, 10 mM, and 20 mM glutathione. The purified fractions were collected, concentrated, and the purity of the protein was assessed on SDS-PAGE (12%) under reducing conditions. The integrity of GST-LRR expression was further confirmed by thrombin treatment. For the purification of GST-LRR mutants (E017A and W139C), we followed the same protocol as GST-LRR WT. All the purification steps were performed at 4°C unless otherwise stated.

Cell proliferation Assays

Effects of GST-LRR on the proliferation efficiency of HEK cells were studied using the freshly purified GST-LRR at varying concentrations (10, 30, 100, and 300 ng/mL). HEK cells were grown in Dulbecco's Modified Eagle Medium (DMEM) as described above. Cell proliferation efficiency was measured by an automatic cell counter (Bio-Rad) for Days 0, 1, 2, and 3. The experiment was performed in a 24-well plate with complete (media + 10% FBS) and incomplete (media only). To harvest the cells, media was aspirated, and cells were washed with PBS. Trypsin (0.05%, 200 ul, Gibco) was added in each target well and incubated it for 5 minutes at room temperature before adding complete DMEM (800 ul) to neutralize the trypsin. Cell counting was performed by mixing 20 ul of the harvested cells with 20 ul of trypan blue. Same protocol was followed for Days 0, 1, and 2 for the effects of E107A and W139C on HEK cells proliferation as well.

Protein Co-Purification Assay

Interaction between GST-LRR and Laminin-511 (AMSBIO, USA) was studied using Co-purification assay as previously studied for several affinity-tagged proteins. (22, 23) Purified GST-LRR WT was incubated with glutathione resins in binding buffer/wash buffer (50 mM Tris-HCl buffer, pH 8.0, 200 mM NaCl, and 1 mM DTT), and the resins were washed after a few minutes with the same buffer to remove the unbound GST-LRR WT. After washing, laminin-511 (~50 ug) was added to the affinity resin already bound with GST-LRR and incubated for 2 h at 4°C. Subsequently, resins were washed twice with binding buffer to remove the non-specific interactions between the proteins and finally the complex was eluted with an elution buffer containing 20 mM reduced glutathione. We followed the same procedure for E107A and W139C mutants for this study as well.

Statistical Analysis

Descriptive data were presented as means \pm SEM. All experiments were repeated at least three times. Prism 8 (GraphPad software) and excel was used to analyze and present the data. Statistical comparison between two groups of data were made using two-tailed unpaired Student's t-test. χ^2 test was used to analyze the statistical significance across groups in zebrafish morpholino studies by comparing relative ratio of each category of curvature between groups. $p < 0.05$ was considered as statistically significant.

Results

*Zebrafish Human PKD1 Paralogs, *pkd1a* and *pkd1b*, Have Redundant Functions*

To examine the role of PC1 in cystogenesis, we employed zebrafish as a model because of its ease in genetic manipulation and short life cycle. Zebrafish has two paralog genes to the human *PKD1*, *pkd1a* and *pkd1b*. Zebrafish with both genes knocked down exhibit phenotypes of dorsal axis curvature and cysts in pronephric ducts. (16) Fertilized zebrafish embryos at 1 to 4 cell stage were injected with previously validated anti-sense morpholinos targeting either *pkd1a* or *pkd1b*. (16) As reported, *pkd1a* and *pkd1b* are redundant and knockdown of both were required for full exhibition of dorsal axis curvature (Figure 1A-C). Around 14% of *pkd1a* morpholino injected embryos showed only mild dorsal tail curvature ($<90^\circ$ relative to body axis) at ~3 days post fertilization (dpf) while there were no detectable phenotypes in morphants injected with *pkd1b* morpholino (Figure 1A-B). Co-injection of both *pkd1a* and *pkd1b* morpholinos resulted in *pkd1a/b* morphants with more severe dorsally curved body axis (Figure 1A-C). Due to dilution and uneven distribution of oligonucleotides among rapid dividing cells, the severity of phenotypes varies among individual embryos. For phenotypic analysis, they were segregated into severe ($>180^\circ$), moderate (90° - 180°), mild ($<90^\circ$) and normal categories (no curvature) based on the degree of curvature (Figure 1C).

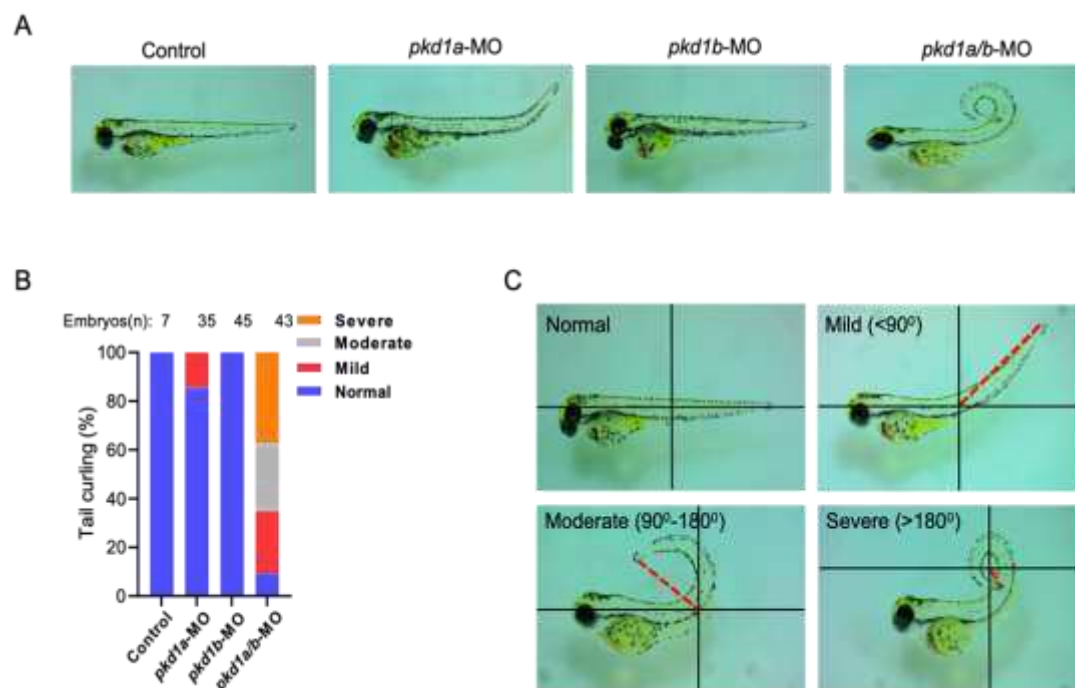


Figure 1. Knockdown of both *pkd1a* and *pkd1b* genes results in dorsal axis curvature in zebrafish embryos. **(A)** Shows uninjected control ZF embryos and embryos injected with either *pkd1a*, *pkd1b* or both morpholinos at ~3 days post fertilization (dpf). *Pkd1a* and *pkd1b* genes are shown to be redundant with no drastic effects when injected alone while combined knockdown results in embryos with varying degree of dorsal axis curvatures. **(B)** Shows percentage of *pkd1a/b*-morphant ZF embryos segregated based on tail curvatures in groups injected with vehicle or morpholinos for *pkd1a*, *pkd1b* or both. The total number (n) of embryos from combined multiple experiments are shown on top. **(C)** Images of ZF morphants deficient for both *pkd1a* and *pkd1b* based on the degree of dorsal body axis curvature at ~3 dpf. Embryos were segregated as normal (no curvature), mild (<90°), moderate (90-180°), and severe (>180°) based on the tail curvature.

Overexpression of N-Terminal Leucine-Rich Repeats Suppresses Dorsal Axis Curvature and Pronephric Cystic Phenotypes in pkd1a/b Morphants

We examined the role of whole extracellular N-terminus of PC1 and LRR in reversing PC1-deficient phenotypes (Figure 2A). mRNA coding for full-length PC1 ("PC1-FL"), the entire extracellular domain ("PC1-ECD") or LRR ("PC1-LRR") were co-injected into zebrafish embryos along with *pkd1a* and *-b* morpholinos. Supporting that dorsal axis curvature in *pkd1a/b* morphant embryos is due to loss of PC1 function, re-expressing full-length human PC1 significantly suppresses dorsal tail curvature (Figure 2B). However, tail curling in *pkd1a/b* morphants is not reversed by injecting an equal amount (200pg) of mRNA expressing the ECD of PC1. Interestingly, co-injecting same amount of mRNA expressing LRR significantly suppressed dorsal tail curvature in the morphant embryos. The amino acid sequence of FL and ECD (4303 and 3074 amino acids) is much longer than LRR (176 amino acids). In these experiments, the number of protein molecules for LRR may be as high as 25-fold more than FL-PC1. We performed dose-dependent studies on effect of LRR on reversing PC1-deficiency. Injecting 1/20th amount of LRR (10 pg) did not reverse dorsal curvature in *pkd1a/b* morphant as 200pg LRR (Figure 2C). Expressing ER-targeted LRR ("LRR-KDEL") even at 200pg had no effect on suppress tail curling in *pkd1a/b* morphants, indicating that extracellular secretion of LRR is necessary for rescuing of tail curling in PC1-deficient zebrafish embryos.

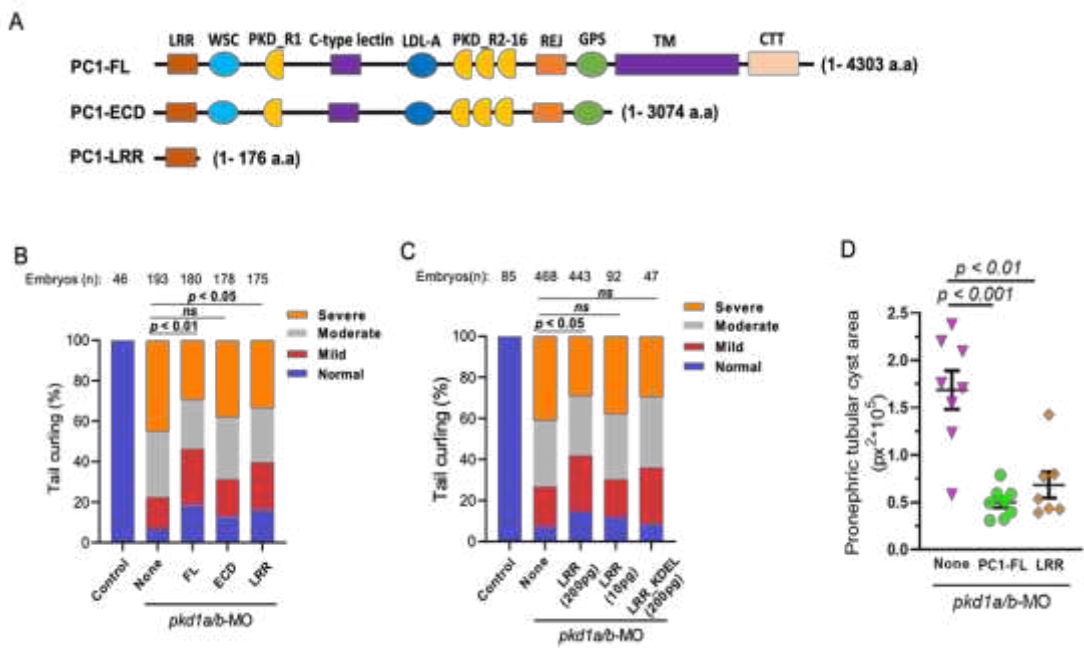


Figure 2. LRR suppresses cystic phenotypes in PC1-morphant zebrafish embryos. **(A)** Diagrammatic presentation of PC1 full length (PC1-FL), truncated extracellular domain (PC1-ECD) and LRR (PC1-LRR) domain alone. **(B)** Shows percentage of *pkd1a/b*-morphant ZF embryos segregated based on severity of tail curling in groups injected with *pkd1a/b*-morpholino along with vehicle (None) or mRNA expressing PC1-FL, ECD or LRR alone. Unlike ECD, co-injection of LRR significantly rescued tail curvature like that of FL. Statistical significance was calculated by comparing relative ratio of each category between groups by Chi-square test. **(C)** Transgenic expression of LRR domain rescued the tail curvature phenotype in *pkd1a/b*-morphant ZF embryos in a dose dependent manner. While expression of ER targeted LRR_KDEL mutant does not rescue. **(D)** Pronephric tubular cyst areas are quantitated in *pkd1a/b*-MO ZF embryos injected with *pkd1a/b* morpholino along with vehicle (None, n=8) or mRNA expressing FL (n=8) or LRR domain (n=7). Cystic area is presented as pixel square (px²). Data are presented as mean ± SEM. Data presented are from at least 3 independent experiments. The total number (n) of embryos from combined multiple experiments are shown on top. Statistical analysis was performed by chi-square test or t-test.

In addition to dorsal axis curvature, the severity of pronephric tubular cysts in *pkd1a/b* morphants were analyzed which is previously shown to correlate with degree of curling (Figure 2D). (24) Embryos injected with *pkd1a/b* morpholino alone (None) exhibited enlarged pronephric tubular cysts. In comparison, *pkd1a/b* morphants co-injected with mRNA for FL-PC1 or LRR significantly suppressed pronephric tubular cyst area in agreement with rescue of tail curling.

LRR Plays an Anti-Proliferative Role in Cell Proliferation

So far, transgenic expression of LRR domain in ZF embryos support its anti-cystogenic effect by suppressing dorsal tail curvature and pronephric cyst area. A previous study reported that LRR plays a suppressive role in cell proliferation. (25) We used HEK293 cells as an *in vitro* model to validate the effect of LRR. Purified LRR domain were added to the culture media of proliferating HEK293 cells at different concentrations ranging from 10 ng/ml to 300 ng/ml (Figure 3A-B). At low dosage (10, 30, 100 ng/ml) LRR tended to decrease cell proliferation rate compared to no LRR, but the effects were not statistically significant. However, cell proliferation was significantly inhibited at 300 ng/ml LRR at Day 2 and 3. Thus, LRR causes a dose dependent inhibition of cell proliferation of HEK cells in culture.

LRR Binds to Extracellular Matrix Protein, Laminin-511

A

LRR₂₄₋₁₇₆

Laminin 511 (E8)

- Laminin α5
- Laminin β1
- Laminin γ1

B

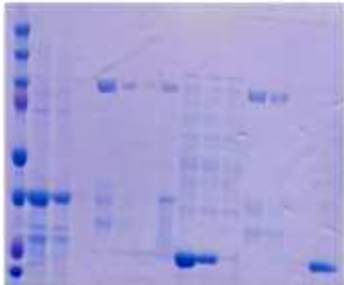
GST-LRR							GST							
L	1	2	3	4	5	6	7	1	2	3	4	5	6	7
														← Laminin 511
														← GST-LRR
														← GST

Figure 4. LRR binds to an extracellular matrix protein Laminin-511 **(A)** *In silico* analysis suggests a molecular interaction between LRR domain and E8 fragment of heterotrimeric laminin 511 composed of laminin $\alpha 5$, laminin $\beta 1$ and laminin $\gamma 1$ chains. **(B)** Co-purification of Laminin 511 along with GST-LRR suggests a physical interaction. GST-tag alone was used as negative control. M= Protein marker, 1= Loading sample, 2= Flow through, 3= Wash, 4= Lamin511 loading sample, 5= Flow through, 6= Washing of laminin after 1 hour incubation, 7= Co-elution of GST-LRR or GST (or GST-LRR mutant

E107A or W139C in Figure 5B) with laminin. Representative data shown are from 3 independent experiments.

Molecular docking identifies amino acid glutamate-107 (E107) and tryptophan-139 (W139) of LRR may be important for interacting with laminin-511. E107 in LRR interacts with arginine-3079 (R3079) of α 5-chain in laminin-511 through hydrogen bonding (Figure 5A). W139 forms hydrogen bonds with glutamine-143 (Q143) and tryptophan-135 (W135) within LRR, which is important for tertiary structure for interaction with laminin-511 (Figure 5A). To substantiate the findings of molecular docking, we examined LRR-laminin-511 interaction by mutating these amino acid residues in the LRR domain. In contrast to WT LRR, laminin-511 did not copurify with GST-tagged LRR carrying E107A mutation (Figure 5B, upper panel). Similarly, LRR domain with W139C mutation showed reduced interaction with laminin 511 (Figure 5B, lower panel). Moreover, application of LRR_E107A or LRR_W139C to the cultured cells exerted a lesser suppression on cell proliferation relative to WT LRR (Figure 5C-D). At day 2, there was a significant difference in the rate of cell proliferation between cells treated with WT LRR and LRR_E107A or LRR_W139C. The results support the notion that interaction between LRR and laminin-511 modulates cell proliferation.

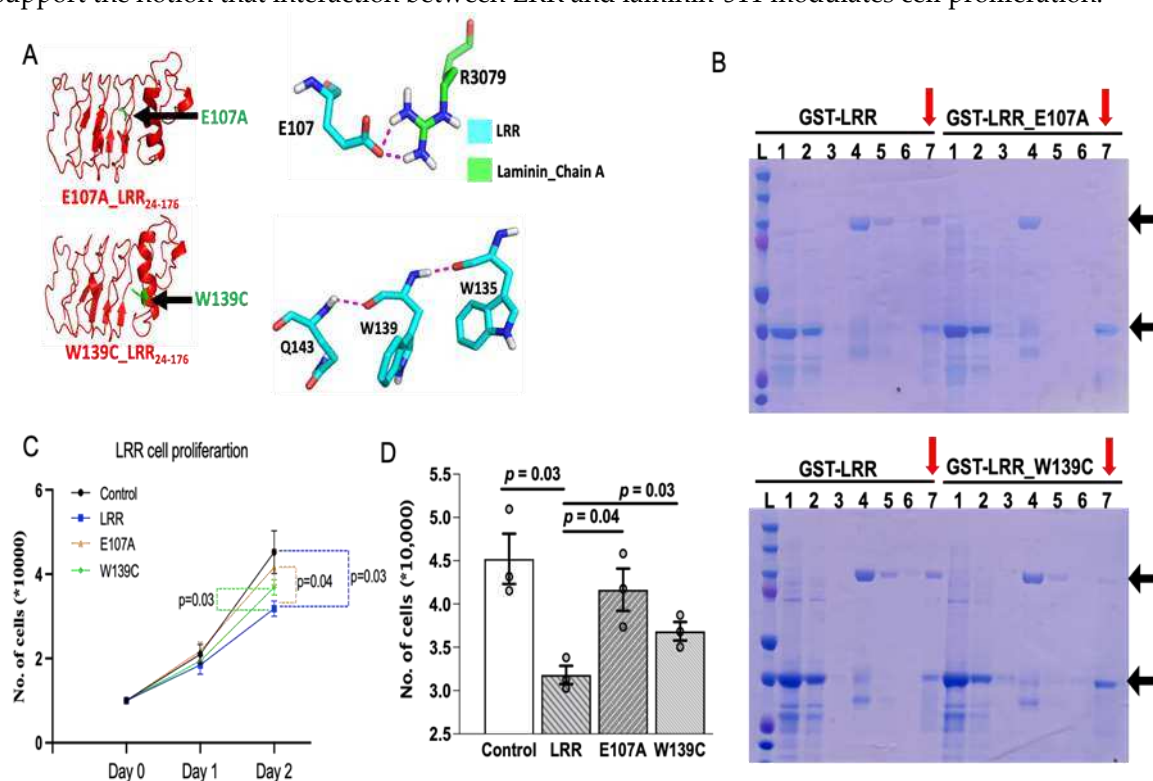


Figure 5. LRR mediates its anti-proliferative effect by regulating PC1-Laminin interaction. (A) (Upper panel) Structural analysis predicts glutamate residue at E107 of LRR domain interacts with arginine residue at 3079 of α 5 chain in laminin 511. Similarly, LRR residue tryptophan at 139 (lower panel), an ADPKD pathogenic variant was found to be in a crucial α -helix conformation with Q143 and W135, alteration of which may hinder LRR-Laminin interaction. (B) Unlike LRR, laminin 511 was not copurified along with E107A and W139C mutants. M= Protein marker, 1= Loading sample, 2= Flow through, 3= Wash, 4= Loading of Lamin511_Trimers, 5= Flow through, 6= Washing of laminin after 1 hour incubation, 7= Co-elution of GST-LRR/GST/E107A/W139C and laminin. Representative data shown are from 3 independent experiments. (C) & (D) Shows cell proliferation is significantly inhibited by addition of LRR (300 ng/ml) at Day 2 but not by E107A and W139C mutants. Data shown are from at least 3 independent experiments. Data are presented as mean \pm SEM.

Binding of LRR to Laminin-511 Suppresses Renal Cystogenesis

We next examine the role of LRR-laminin-511 interaction to ameliorate renal cystogenesis using *pkd1a/b* zebrafish morphants as described previously. mRNA expressing full-length PC1, WT LRR

or LRR mutants (E107A or W139C) were co-injected with *pkd1a/b* morpholinos. Dorsal axis curvature and pronephric cystogenesis were analyzed at ~3 dpf (Figure 6). As reported earlier, injection of mRNAs expressing full-length PC1 or WT LRR (at 200pg each) significantly suppressed dorsal tail curvature in *pkd1a/b* morphants (Figure 6A). However, co-injecting LRR mutants, E107A or W139C along with *pkd1a/b* morpholinos did not reverse tail curvature in ZF embryos. Likewise, total cystic area in pronephric tubules in *pkd1a/b* morphants were reduced by WT LRR but considerably less so by E107A or W139C LRR mutants (Figure 6B). Thus, disruption of LRR-laminin interaction by mutation of critical residues in the LRR domain impairs the anti-cystogenic effect of LRR.

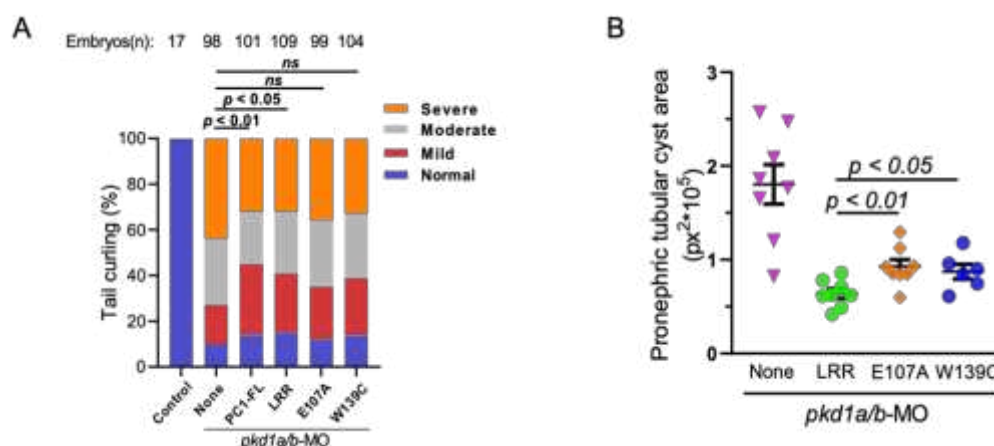


Figure 6. LRR-Laminin interaction is necessary for anti-cystogenic effect of LRR. **(A)** Shows transgenic expression of PKD1 or LRR rescues tail curvature phenotype in *pkd1*-morphant ZF embryos while both E107A and W139C-LRR mutants does not. Data presented are from at least 3 independent experiments. The total number (n) of embryos from combined multiple experiments are shown on top. Statistical analysis was performed by chi-square test. **(B)** Pronephric tubular cyst areas are quantitated in vehicle (None), LRR, E107A or W139C expressed ZF embryos co-injected with *pkd1a/b* morpholinos. Total cystic area is significantly reduced in LRR expressed *pkd1*-MO ZF embryos but not with E107A and W139C. Cystic area is presented as pixel square (px²). Data are presented as mean ± SEM.

Discussion

Mutations of PC1 accounts for majority of ADPKD cases. How PC1 exerts anti-cystogenesis remains poorly understood. The transmembrane (TM) domain of PC1 participates in the formation of channel complexes with PC2. (5) The intracellular C-terminus is reported to be involved in interaction and regulation of many intracellular signaling pathways and is translocated to nucleus as well as mitochondria to regulate gene transcription and mitochondrial function. (4, 6, 30, 31) The role of ~3000 amino acid long N-terminal extracellular domain of PC1 (ECD) in disease pathogenesis is highlighted by the fact that many pathogenic variants in PKD1 with clinical significance lie in the region. In addition to the primary cilium and endoplasmic reticulum, PC1 is expressed in the basolateral membrane. Many studies have reported interaction of ECD of PC1 with extracellular matrix (ECM). (26, 32) Altered matrix integrity and anomalous expression of ECM proteins such as collagen, proteoglycans, focal adhesion protein tensin, laminin and integrins are noted in ADPKD. (26, 33) Similarly, polycystic cells derived from PKD mice are shown to have excessive adhesion to ECM proteins. (34) These abnormal cell-matrix interactions in PKD are believed contributing to altered renal epithelial cell proliferation and cystogenesis.

In the current study we explored the role of ECD of PC1 in the development of kidney cysts in ADPKD using a zebrafish model. We found that the entire ECD not capable of substituting the effect of full-length PC1 to reverse PC1-deficient phenotypes in zebrafish. Interestingly, the LRR domain in the absence of rest of ECD is capable of reversing PC1-deficiency when it is overexpressed. The effects of LRR are demonstrated by reversal of dorsal axis curvature and pronephric cystic area, both well-characterized to represent PC1 function in zebrafish. The effect of LRR acting from the extracellular

space is supported by the finding that ER-targeted LRR (LRR_KDEL, Figure 2C) has no effects. The observation that expression of truncated membrane-free ECD does not rescue PC1-deficient phenotypes whereas expression of full-length membranous-anchored PC1 has effect is likely because ECD has much lower local effective concentration when expressed as an extracellularly secreted peptide. At the same dosage of mRNA injected, isolated LRR is ~17-fold molar excess than ECD, thus underscoring isolated LRR is effective. Importantly, in the native state, the LRR domain is attached to PC1 anchored to the cell membrane. The local effective concentration of LRR in the context of PC1 in the native tissue thus is likely much higher than when expressed as an isolated domain.

A previous study by Malhas *et al.* reported that LRR domain binds to extracellular matrix proteins including laminin, collagen, and fibronectin. (25) Laminins are extracellular matrix glycoproteins which make up a major component of the basement membrane. They are an important and biologically active part of the basal lamina on which cells sit that can influence cell differentiation, migration, and adhesion. (35, 36) Laminins are heterotrimeric consisting of three different chains, α , β and γ . Many cell types (including HEK cells used in the study) secrete laminins when grown in cell culture; cell interaction with the secreted laminins affects cell behavior. To investigate the mechanism by which LRR may be involved in anti-cystogenesis, we first demonstrate that extracellular application of LRR inhibits proliferation of HEK cells which secrete laminin that consists of $\alpha 5$, $\beta 1$ and $\gamma 1$ chain (i.e., laminin-511, also known as laminin 10). (37) We further demonstrate that LRR binds to laminin-511 in vitro. Moreover, mutating key residues in the LRR domain important for binding laminin-511 diminishes its ability to inhibit HEK cell proliferation and to suppress pronephric cystogenesis in PC1-deficient zebrafish embryos. With respects to how LRR binding to laminin-511 affects cell proliferation, cells interacts with laminin through cell membrane receptor integrins. HEK cells express endogenous integrin $\alpha 6 \beta 1$ which are known receptors for laminin-511. (18, 38, 39) Binding to laminin through cell membrane integrin receptors activates EGFR tyrosine phosphorylation and MAPK phosphorylation to regulate cell proliferation. (39) Thus, LRR may inhibit HEK cell proliferation by binding and competing laminin-511 interaction with integrin $\alpha 6 \beta 1$ on HEK cell membrane (Figure 7).

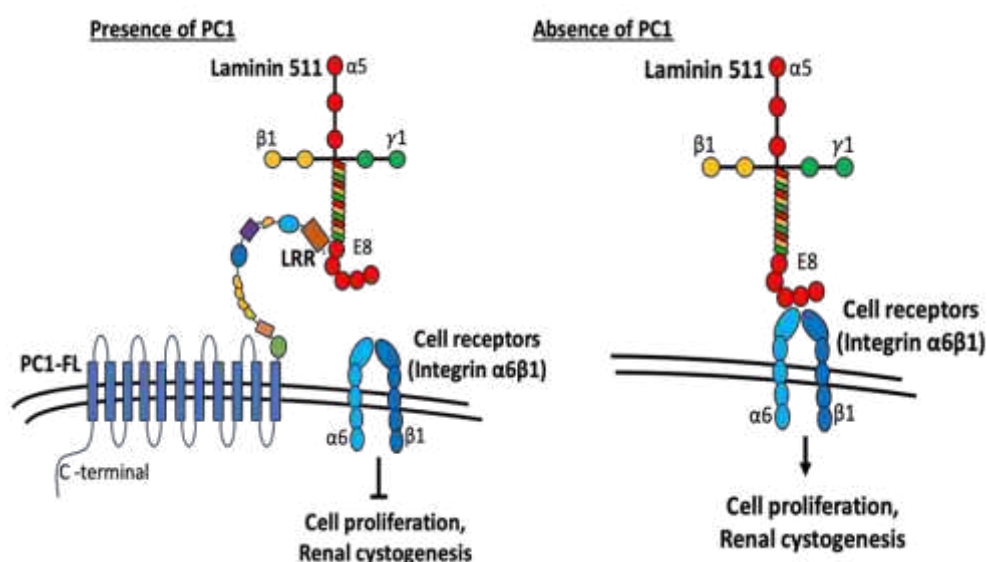


Figure 7. Working model depicting the role of LRR in modulating cell proliferation and cystogenesis. Current work suggests the role of PC1 as a modulator of ECM components. N-terminal extracellular fragment of PC1 contains multiple domains similar to various adhesion proteins that are involved in cell-cell and cell-matrix contacts. LRR domains in PC1 interacts with laminin 511 and inhibits its interaction with cell surface receptors integrin $\alpha 6 \beta 1$. Without PC1, laminin-511 interacts with integrin $\alpha 6 \beta 1$ to trigger downstream signaling cascades promoting cell proliferation and renal cystogenesis. See text for more details.

Similar mechanism likely explains how LRR exerts anti-cystogenesis effect in the kidney (Figure 7). Laminin-511 is the predominant basement membranes component for renal tubules. (40) LRR domain of PC1 in the basal membrane of renal tubular cells may modulate cell-matrix contact between tubular epithelial cells and basement membrane to suppress intercellular events leading to cystogenesis including cell proliferation. In support of the hypothesis, laminin is shown to influence the identity of polycystic tubular epithelial cells. (26) Evidence also exists for alterations in laminin expression leads to PKD. Shannon *et al.* have shown that expression of truncated laminin $\alpha 5$ chain leads to cysts and renal failure in mice. (41) As above, integrins are cell surface receptors for laminin. Integrin binding to laminin will activate intracellular signaling (see below) leading to cell proliferation. We propose that LRR binding to laminin would prevent its interaction with integrins and suppress proliferation and other processes of cystogenesis. In support for the notion, Lee *et al.* report that integrin signaling is upregulated in *Pkd1*-deleted mice and deletion of integrin ameliorates cystogenesis and improves the renal function in these mice. (42) Thus, PC1 may act as an inhibitor of integrin mediated signaling through regulating ECM-integrin crosstalk. Activation of integrin receptors leads to increased PI3K, Ca^{2+} level and Ras/Raf/Erk signaling pathways all of which may be associated with ADPKD. Furthermore, PC1 colocalizes with integrin proteins in focal adhesions, cell-cell contact and cilium in renal epithelial cells. (26, 43, 44) It is also reported that polycystic cells exhibit increased adhesion to laminin proteins through integrins, (34) further supporting that PC1 exerts integrin-ECM interaction. Along the same line, laminin-332 and its binding partner integrin $\alpha 6\beta 4$ are altered in PKD. (33) Thus, LRR of PC1 present in the basolateral membrane may regulate cell-matrix and cell-cell interactions through affecting cell surface integrin receptors binding with laminin imbedded in the basement membrane or secreted between cells. Disturbances in these processes may alter cell proliferation, cell adhesion and tissue architecture underlie the pathogenesis of ADPKD.

Finally, besides LRR other domains in the extracellular region of PC1 also bind proteins in the ECM and regulate cell-cell/matrix interaction. For instance, C-type lectin domain in the ECD of PC1 is shown to interact with Type I, II and IV collagens as well as laminin proteins. It binds to carbohydrate residues in these proteins in a dose dependent manner and may regulate cell-cell signaling. (26) Likewise, Ig-like PKD repeats in the ECD have strong homophilic interactions and antibodies against these domains disrupts cell-cell contacts by reducing intercellular adhesion. (32) Our present study supports the view that altered ECM components by PC1 deficiency contributes to the pathogenesis of ADPKD. Other regions of PC1 undoubtedly also play important roles in the function of PC1 in anti-cystogenesis, such as the role of TM of PC1 forming channel complex with PC2 and the role of the C-terminal intracellular tail in regulating gene transcription as well as mitochondrial function. (4-6, 30, 31)

Author Contributions: B.P., M.A., and J.X. designed the study, conducted the experiments, analyzed the data, and participated in writing the paper; C.-L.H. supervised the entire project and edited the manuscript. All authors approved the final version of the submitted manuscript.

Funding: This work was supported, in part, by the National Institutes of Health, National Institute of Diabetes and Digestive and Kidney Diseases (DK109887 to C.-L. Huang).

Institutional Review Board Statement:

Informed Consent Statement:

Data availability statement: The data that support the findings of this study are available on request from the corresponding author.

Conflicts of Interest: C.-L. Huang reports holding the Roy J. Carver Chair in Internal Medicine in the University of Iowa Carver College of Medicine. This work was supported, in part, by philanthropic gifts from Jared and Carol Hills. All remaining authors have nothing to disclose.

References

- Luciano, R. L., and Dahl, N. K. (2014) Extra-renal manifestations of autosomal dominant polycystic kidney disease (ADPKD): considerations for routine screening and management. *Nephrol Dial Transplant* **29**, 247-254
- Igarashi, P., and Somlo, S. (2002) Genetics and pathogenesis of polycystic kidney disease. *J Am Soc Nephrol* **13**, 2384-2398
- Grimm, D. H., Cai, Y., Chauvet, V., Rajendran, V., Zeltner, R., Geng, L., Avner, E. D., Sweeney, W., Somlo, S., and Caplan, M. J. (2003) Polycystin-1 distribution is modulated by polycystin-2 expression in mammalian cells. *J Biol Chem* **278**, 36786-36793
- Lin, C. C., Kurashige, M., Liu, Y., Terabayashi, T., Ishimoto, Y., Wang, T., Choudhary, V., Hobbs, R., Liu, L. K., Lee, P. H., Outeda, P., Zhou, F., Restifo, N. P., Watnick, T., Kawano, H., Horie, S., Prinz, W., Xu, H., Menezes, L. F., and Germino, G. G. (2018) A cleavage product of Polycystin-1 is a mitochondrial matrix protein that affects mitochondria morphology and function when heterologously expressed. *Sci Rep* **8**, 2743
- Su, Q., Hu, F., Ge, X., Lei, J., Yu, S., Wang, T., Zhou, Q., Mei, C., and Shi, Y. (2018) Structure of the human PKD1-PKD2 complex. *Science* **361**
- Low, S. H., Vasanth, S., Larson, C. H., Mukherjee, S., Sharma, N., Kinter, M. T., Kane, M. E., Obara, T., and Weimbs, T. (2006) Polycystin-1, STAT6, and P100 function in a pathway that transduces ciliary mechanosensation and is activated in polycystic kidney disease. *Dev Cell* **10**, 57-69
- Parnell, S. C., Magenheimer, B. S., Maser, R. L., Rankin, C. A., Smine, A., Okamoto, T., and Calvet, J. P. (1998) The polycystic kidney disease-1 protein, polycystin-1, binds and activates heterotrimeric G-proteins in vitro. *Biochem Biophys Res Commun* **251**, 625-631
- Arnould, T., Kim, E., Tsiokas, L., Jochimsen, F., Gruning, W., Chang, J. D., and Walz, G. (1998) The polycystic kidney disease 1 gene product mediates protein kinase C alpha-dependent and c-Jun N-terminal kinase-dependent activation of the transcription factor AP-1. *J Biol Chem* **273**, 6013-6018
- Casuscelli, J., Schmidt, S., DeGray, B., Petri, E. T., Celic, A., Foltá-Stogniew, E., Ehrlich, B. E., and Boggon, T. J. (2009) Analysis of the cytoplasmic interaction between polycystin-1 and polycystin-2. *Am J Physiol Renal Physiol* **297**, F1310-1315
- Giamarchi, A., Feng, S., Rodat-Despoix, L., Xu, Y., Bubenshchikova, E., Newby, L. J., Hao, J., Gaudioso, C., Crest, M., Lupas, A. N., Honore, E., Williamson, M. P., Obara, T., Ong, A. C., and Delmas, P. (2010) A polycystin-2 (TRPP2) dimerization domain essential for the function of heteromeric polycystin complexes. *EMBO J* **29**, 1176-1191
- Weston, B. S., Malhas, A. N., and Price, R. G. (2003) Structure-function relationships of the extracellular domain of the autosomal dominant polycystic kidney disease-associated protein, polycystin-1. *FEBS Lett* **538**, 8-13
- Harris, P. C., and Torres, V. E. (2009) Polycystic kidney disease. *Annu Rev Med* **60**, 321-337
- Liu, X., Vien, T., Duan, J., Sheu, S. H., DeCaen, P. G., and Clapham, D. E. (2018) Polycystin-2 is an essential ion channel subunit in the primary cilium of the renal collecting duct epithelium. *Elife* **7**
- Caplan, M. J. (2019) Holding open the door reveals a new view of polycystin channel function. *EMBO Rep* **20**, e49156
- Padhy, B., Xie, J., Wang, R., Lin, F., and Huang, C. L. (2022) Channel Function of Polycystin-2 in the Endoplasmic Reticulum Protects against Autosomal Dominant Polycystic Kidney Disease. *J Am Soc Nephrol* **33**, 1501-1516
- Mangos, S., Lam, P. Y., Zhao, A., Liu, Y., Mudumana, S., Vasilyev, A., Liu, A., and Drummond, I. A. (2010) The ADPKD genes *pkd1a/b* and *pkd2* regulate extracellular matrix formation. *Dis Model Mech* **3**, 354-365
- Sullivan-Brown, J., Bisher, M. E., and Burdine, R. D. (2011) Embedding, serial sectioning and staining of zebrafish embryos using JB-4 resin. *Nat Protoc* **6**, 46-55
- Takizawa, M., Arimori, T., Taniguchi, Y., Kitago, Y., Yamashita, E., Takagi, J., and Sekiguchi, K. (2017) Mechanistic basis for the recognition of laminin-511 by alpha6beta1 integrin. *Sci Adv* **3**, e1701497
- Yang, J., and Zhang, Y. (2015) I-TASSER server: new development for protein structure and function predictions. *Nucleic Acids Res* **43**, W174-181
- Yang, J., Yan, R., Roy, A., Xu, D., Poisson, J., and Zhang, Y. (2015) The I-TASSER Suite: protein structure and function prediction. *Nat Methods* **12**, 7-8
- Kozakov, D., Hall, D. R., Xia, B., Porter, K. A., Padhony, D., Yueh, C., Beglov, D., and Vajda, S. (2017) The ClusPro web server for protein-protein docking. *Nat Protoc* **12**, 255-278
- Kaur, J., and Reinhardt, D. P. (2012) Immobilized metal affinity chromatography co-purifies TGF-beta1 with histidine-tagged recombinant extracellular proteins. *PLoS One* **7**, e48629
- Ray, D., Lavery, K. U., Jolma, A., Nie, K., Samson, R., Pour, S. E., Tam, C. L., von Krosigk, N., Nabeel-Shah, S., Albu, M., Zheng, H., Perron, G., Lee, H., Najafabadi, H., Blencowe, B., Greenblatt, J., Morris, Q., and Hughes, T. R. (2023) RNA-binding proteins that lack canonical RNA-binding domains are rarely sequence-specific. *Sci Rep* **13**, 5238

24. Arif Pavel, M., Lv, C., Ng, C., Yang, L., Kashyap, P., Lam, C., Valentino, V., Fung, H. Y., Campbell, T., Moller, S. G., Zenisek, D., Holtzman, N. G., and Yu, Y. (2016) Function and regulation of TRPP2 ion channel revealed by a gain-of-function mutant. *Proc Natl Acad Sci U S A* **113**, E2363-2372
25. Malhas, A. N., Abuknesha, R. A., and Price, R. G. (2002) Interaction of the leucine-rich repeats of polycystin-1 with extracellular matrix proteins: possible role in cell proliferation. *J Am Soc Nephrol* **13**, 19-26
26. Weston, B. S., Bagneris, C., Price, R. G., and Stirling, J. L. (2001) The polycystin-1 C-type lectin domain binds carbohydrate in a calcium-dependent manner, and interacts with extracellular matrix proteins in vitro. *Biochim Biophys Acta* **1536**, 161-176
27. Banerjee, M., Virtanen, I., Palgi, J., Korsgren, O., and Otonkoski, T. (2012) Proliferation and plasticity of human beta cells on physiologically occurring laminin isoforms. *Mol Cell Endocrinol* **355**, 78-86
28. Ido, H., Harada, K., Futaki, S., Hayashi, Y., Nishiuchi, R., Natsuka, Y., Li, S., Wada, Y., Combs, A. C., Ervasti, J. M., and Sekiguchi, K. (2004) Molecular dissection of the alpha-dystroglycan- and integrin-binding sites within the globular domain of human laminin-10. *J Biol Chem* **279**, 10946-10954
29. Kunneken, K., Pohlentz, G., Schmidt-Hederich, A., Odenthal, U., Smyth, N., Peter-Katalinic, J., Bruckner, P., and Eble, J. A. (2004) Recombinant human laminin-5 domains. Effects of heterotrimerization, proteolytic processing, and N-glycosylation on alpha3beta1 integrin binding. *J Biol Chem* **279**, 5184-5193
30. Puri, S., Magenheimer, B. S., Maser, R. L., Ryan, E. M., Zien, C. A., Walker, D. D., Wallace, D. P., Hempson, S. J., and Calvet, J. P. (2004) Polycystin-1 activates the calcineurin/NFAT (nuclear factor of activated T-cells) signaling pathway. *J Biol Chem* **279**, 55455-55464
31. Lal, M., Song, X., Pluznick, J. L., Di Giovanni, V., Merrick, D. M., Rosenblum, N. D., Chauvet, V., Gottardi, C. J., Pei, Y., and Caplan, M. J. (2008) Polycystin-1 C-terminal tail associates with beta-catenin and inhibits canonical Wnt signaling. *Hum Mol Genet* **17**, 3105-3117
32. Ibraghimov-Beskrovnya, O., Bukanov, N. O., Donohue, L. C., Dackowski, W. R., Klinger, K. W., and Landes, G. M. (2000) Strong homophilic interactions of the Ig-like domains of polycystin-1, the protein product of an autosomal dominant polycystic kidney disease gene, PKD1. *Hum Mol Genet* **9**, 1641-1649
33. Joly, D., Morel, V., Hummel, A., Ruella, A., Nusbaum, P., Patey, N., Noel, L. H., Rousselle, P., and Knebelmann, B. (2003) Beta4 integrin and laminin 5 are aberrantly expressed in polycystic kidney disease: role in increased cell adhesion and migration. *Am J Pathol* **163**, 1791-1800
34. van Adelsberg, J. (1994) Murine polycystic kidney epithelial cell lines have increased integrin-mediated adhesion to collagen. *Am J Physiol* **267**, F1082-1093
35. von der Mark, K., and Kuhl, U. (1985) Laminin and its receptor. *Biochim Biophys Acta* **823**, 147-160
36. Yap, L., Tay, H. G., Nguyen, M. T. X., Tjin, M. S., and Tryggvason, K. (2019) Laminins in Cellular Differentiation. *Trends Cell Biol* **29**, 987-1000
37. Nakashima, Y., Kariya, Y., and Miyazaki, K. (2007) The beta3 chain short arm of laminin-332 (laminin-5) induces matrix assembly and cell adhesion activity of laminin-511 (laminin-10). *J Cell Biochem* **100**, 545-556
38. Bodary, S. C., and McLean, J. W. (1990) The integrin beta 1 subunit associates with the vitronectin receptor alpha v subunit to form a novel vitronectin receptor in a human embryonic kidney cell line. *J Biol Chem* **265**, 5938-5941
39. Yarwood, S. J., and Woodgett, J. R. (2001) Extracellular matrix composition determines the transcriptional response to epidermal growth factor receptor activation. *Proc Natl Acad Sci U S A* **98**, 4472-4477
40. Miner, J. H. (1999) Renal basement membrane components. *Kidney Int* **56**, 2016-2024
41. Shannon, M. B., Patton, B. L., Harvey, S. J., and Miner, J. H. (2006) A hypomorphic mutation in the mouse laminin alpha5 gene causes polycystic kidney disease. *J Am Soc Nephrol* **17**, 1913-1922
42. Lee, K., Boctor, S., Barisoni, L. M., and Gusella, G. L. (2015) Inactivation of integrin-beta1 prevents the development of polycystic kidney disease after the loss of polycystin-1. *J Am Soc Nephrol* **26**, 888-895
43. Wilson, P. D., Geng, L., Li, X., and Burrow, C. R. (1999) The PKD1 gene product, "polycystin-1," is a tyrosine-phosphorylated protein that colocalizes with alpha2beta1-integrin in focal clusters in adherent renal epithelia. *Lab Invest* **79**, 1311-1323
44. Drummond, I. A. (2011) Polycystins, focal adhesions and extracellular matrix interactions. *Biochim Biophys Acta* **1812**, 1322-1326

Disclaimer/Publisher's Note: The statements, opinions and data contained in all publications are solely those of the individual author(s) and contributor(s) and not of MDPI and/or the editor(s). MDPI and/or the editor(s) disclaim responsibility for any injury to people or property resulting from any ideas, methods, instructions or products referred to in the content.